# Reaction Mechanisms Displayed by Catalytic Antibodies

JON D. STEWART, LOUIS J. LIOTTA, AND STEPHEN J. BENKOVIC*

*Department of Chemistry, The Pennsylvania State University, 152 Davey Laboratory, University Park, Pennsylvania 16802*

*Received April 6, 1993*

The field of catalytic antibodies now encompasses some 50 examples of various chemical reactions catalyzed by antibodies that have been induced to compounds (haptens) that mimic either the transition states or the high-energy intermediates encountered in those chemical transformations.[1-3] The creation of the "active site" is a consequence of the immunological response to the hapten's structure and will reflect the diversity of solutions to optimizing the molecular interactions between side chain and backbone elements derived from the peptidic antibody framework and complementary regions of the hapten. A central question is the extent to which this response engenders an active site that exhibits the sophisticated catalytic refinements possessed by enzymes that have presumably been optimized by evolution. In this article, we focus on a selected subset of antibody-catalyzed reactions for which there is an appreciable body of evidence for their likely mechanistic course. Although some features clearly are programmed by the inducing hapten, others rich in kinetic and stereochemical complexity appear to arise as a consequence of the chemistry within a confined space walled by protein. Thus, we find and describe reoccurring mechanistic themes displaying characteristics previously associated with enzyme behavior, e.g. multistep substrate processing, induced fit, and allosteric modulation. Instructed by such analogies, we suggest various means for extending the scope and increasing the reactivity of catalytic antibodies (abzymes).

## Hydrolytic Reactions

The ability to cleave peptide bonds site-specifically constitutes an important goal of abzyme research since such catalysts would have many potential applications in controlling biological systems. While amide hydrolysis is a thermodynamically favorable process, the reaction possesses an appreciable kinetic barrier since the half-life of a nonactivated amide bond at neutral pH has recently been estimated as approximately 7 years.[4] However, by employing combinations of nucleophilic, acid-base, or metal ion-assisted mechanisms, proteolytic enzymes increase this rate by factors up to $10^{10}$.[5] In all cases, the reaction proceeds through one or more high-energy tetrahedral transition states. Stable compounds that mimic the geometric and electronic characteristics of these high-energy intermediates have proven to be potent competitive inhibitors.[6] In particular, substrate analogs in which the reactive carbonyl has been replaced by either a charged tetrahedral phosphorus or a secondary alcohol have found wide applicability in the rational design of protease inhibitors.[7,8]

These principles have also been applied to produce transition-state mimics that elicit antibodies with esterase and amidase activities.[9] Specifically, an antigen (hapten) patterned after a potent protease inhibitor is chosen for immunization in order to elicit an antibody binding pocket that is complementary to the transition-state or high-energy intermediate that occurs during the corresponding ester or amide hydrolysis. In practice, the actual catalytic mechanism followed by the antibody may be more complex than that envisioned in the hapten design and an example of this is discussed below.

Antibody 43C9, raised against phosphonamidate 1, accelerates the hydrolysis of amide 2 by a factor of approximately $1 \times 10^6$ at pH 9.0, making it one of the most efficient abzymes known (Scheme I).[10] The same antibody also catalyzes the hydrolysis of a series of esters (**3a-e**). While the hapten was designed to favor either nucleophilic or general base catalysis by solvent, the kinetic analysis argued for a more complex mechanism involving an antibody-bound intermediate.[11] Subsequent steady-state and pre-steady-state kinetic studies were also consistent with the idea that hydrolysis of both the amide and the esters proceeds through a transient, antibody-bound intermediate which does not accumulate because of an unfavorable equilibrium that governs its formation. Measurement of $H_2{}^{18}O$ incor-

Jon Stewart, born in Elmira, NY, in 1964, received both his B.S. and M.S. degrees in chemistry from Bucknell University. He then obtained a Ph.D. degree from Cornell University under the supervision of Professor Bruce Ganem in 1991. He is currently a Helen Hay Whitney Foundation postdoctoral fellow in Professor Benkovic's laboratory where he applies the technique of protein engineering to catalytic antibodies. He has accepted a faculty position in the Department of Chemistry at the University of Florida.

Louis J. Liotta was born in Elizabeth, NJ, in 1963. He earned his B.S. in chemistry from The Pennsylvania State University in 1985 and his Ph.D. in Organic Chemistry from Cornell University (with B. Ganem) in 1990. He is currently an NIH postdoctoral fellow in the laboratory of S. J. Benkovic at The Pennsylvania State University. He will join the faculty at Stonehill College, MA, in August 1993.

Stephen J. Benkovic was born in Orange, NJ, and received his undergraduate degree at Lehigh and his Ph.D. at Cornell. After a period as a postdoctoral research associate at UC-Santa Barbara, he joined the faculty at Penn State University in 1965. He now holds the rank of Evan Pugh Professor and the Eberly Chair in Chemistry. He has been recognized by numerous national and international awards and was elected a member of the National Academy of Science in 1985.

(1) Lerner, R. A.; Benkovic, S. J.; Schultz, P. G. *Science* **1991**, *252*, 659-667.
(2) Benkovic, S. J. *Annu. Rev. Biochem.* **1992**, *61*, 29-54.
(3) Hilvert, D. *Pure Appl. Chem.* **1992**, *64*, 1103-1108.
(4) Kahne, D.; Still, W. C. *J. Am. Chem. Soc.* **1988**, *110*, 7529-7534.
(5) Corey, D. R.; Craik, C. S. *J. Am. Chem. Soc.* **1992**, *114*, 1784-1790.
(6) Wolfenden, R. *Acc. Chem. Res.* **1972**, *5*, 10-18.
(7) Bartlett, P. A.; Marlowe, C. K. *Biochemistry* **1983**, *22*, 4618-4624.
(8) Vara Prasad, J. V. N.; Rich, D. H. *Tetrahedron Lett.* **1990**, *31*, 1803-1806.
(9) Stewart, J. D.; Benkovic, S. J. *Chem. Soc. Rev.* **1993**, in press.
(10) Janda, K. D.; Schloeder, D.; Benkovic, S. J.; Lerner, R. A. *Science* **1988**, *241*, 1188-1191.
(11) Benkovic, S. J.; Adams, J. A.; Borders, C. L., Jr.; Janda, K. D.; Lerner, R. A. *Science* **1990**, *250*, 1135-1139.

0001-4842/93/0126-0396$04.00/0 

**Scheme I**

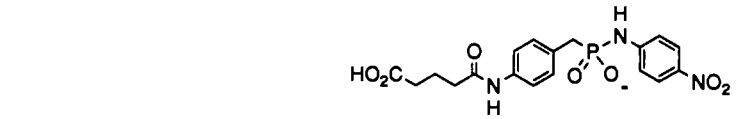

1

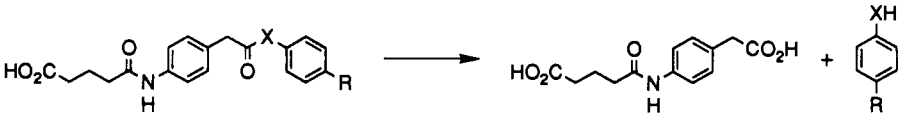

2 X = NH, R = $NO_2$

3 a X = O, R = $NO_2$
b X = O, R = Cl
c X = O, R = $COCH_3$
d X = O, R = CHO
e X = O, R = $CH_3$

4

5 X = NH, R = $NO_2$

6 a X = O, R = $NO_2$
b X = O, R = Cl
c X = O, R = $COCH_3$
d X = O, R = CHO
e X = O, R = $CH_3$

poration[12] and establishment of a structure–reactivity correlation for ester hydrolysis (a Hammet $\sigma$–$\rho$ plot) suggested that this intermediate was an acyl–antibody formed by nucleophilic attack of a histidine side chain on the substrate.[13] Cloning the DNA encoding 43C9 revealed that the protein contained two histidines, one in the light chain and one in the heavy chain.[14] *A priori*, one or both of these might play roles in the kinetic mechanism of 43C9. To support or refute our hypothesis that an acyl–imidazole was the key catalytic intermediate, we sought to use the techniques of site-directed mutagenesis to probe the role of this and other residues of 43C9.

In the absence of high-resolution structural data for 43C9, a computer model of its Fv fragment was constructed in order to guide the mutagenesis experiments.[15] This approach is feasible because the overall fold of antibodies with diverse ligand specificities appears to be highly conserved with differences generally confined to the lengths and conformations of the six complementarity-determining regions (CDR loops). The computer model of 43C9 was constructed in several steps. First, a data base of light and heavy chain conformations was constructed on the basis of published antibody crystal structures, then the amino acid sequence of 43C9 was compared to those in the data base in order to match them with the most closely-related partners within the ensemble of known structures. The light-chain sequence of 43C9 was found to be most similar to that of antiphosphocholine antibody McPC603 and the heavy chain of 43C9 most closely resembled the anti-lysozyme antibody D1.3. Starting from these structures, the appropriate amino acids were altered to "mutate" these starting sequences into that of 43C9, then the two chains of 43C9 were superimposed onto those of structurally characterized Fv fragments in order to properly orient the two chains with respect to one another. Finally, a combination of manual adjustment and energy minimization was used to relieve steric congestion between residues and, in particular, between the heavy and light chains at the $V_L/V_H$ interface.

This model suggested that the surface of 43C9 contains a T-shaped groove which represents a likely location for both hapten binding and catalytic activity. It was possible to dock the hapten into this model cleft with some confidence by virtue of an arginine residue exposed at the bottom of the pocket. This arginine residue represents a conserved feature of antibodies that bind phosphorus oxyanions where the side chain guanidinium group makes both hydrogen-bonding and electrostatic interactions with the ligand. Using this criterion, the phosphonamidate of hapten 1 was placed in the antigen-binding site above the side chain of arginine L96 and the docked structure manipulated to minimize any steric clash between the aromatic side chains of the hapten and the walls of the binding pocket (Figure 1).

This location for hapten immediately suggested key roles for two residues in the catalytic mechanism of 43C9: histidine L91 and arginine L96. The imidazole side chain of His L91 is oriented parallel to the guanidinium group of Arg L96, and the closer ring nitrogen is located approximately 3 Å from the carbonyl mimic of the hapten. This proximity, coupled with the structure reactivity correlation, suggested that His L91 might act as the active site nucleophile. The other histidine, His H35, which appears to play a role in maintaining the structure of the third CDR loop of the heavy chain, is located approximately 7 Å from the phosphorus atom of hapten 1. The placement of the guanidinium group of Arg L96 suggested that it might function to stabilize the anionic tetrahedral intermediates formed during turnover.

Antibody 43C9 was cloned in single-chain antibody form to facilitate site-directed mutagenesis and protein overexpression in *Escherichia coli*.[13] In this construct, the DNA encodes only the variable regions of the light and heavy chains joined by a 14 amino acid linker, thus reducing the size of the antibody from 150 to 27 kDa. Importantly, the kinetic constants for the hydrolysis of

(12) Janda, K. D.; Ashley, J. A.; Jones, T. M.; McLeod, D. A.; Schloeder, D. M.; Weinhouse, M. I.; Lerner, R. A.; Gibbs, R. A.; Benkovic, P. A.; Hilhorst, R.; Benkovic, S. J. *J. Am. Chem. Soc.* **1991**, *113*, 291–297.

(13) Gibbs, R. A.; Benkovic, P. A.; Janda, K. D.; Lerner, R. A.; Benkovic, S. J. *J. Am. Chem. Soc.* **1992**, *114*, 3528–3534.

(14) Gibbs, R. A.; Posner, B. A.; Filpula, D. R.; Dodd, S. W.; Finkelman, M. A. J.; Lee, T. K.; Wroble, M.; Whitlow, M.; Benkovic, S. J. *Proc. Natl. Acad. Sci. U.S.A.* **1991**, *88*, 4001–4004.

(15) Roberts, V. A.; Stewart, J. D.; Benkovic, S. J.; Getzoff, E. D. *J. Mol. Biol.* **1993**, submitted.

**Scheme II**

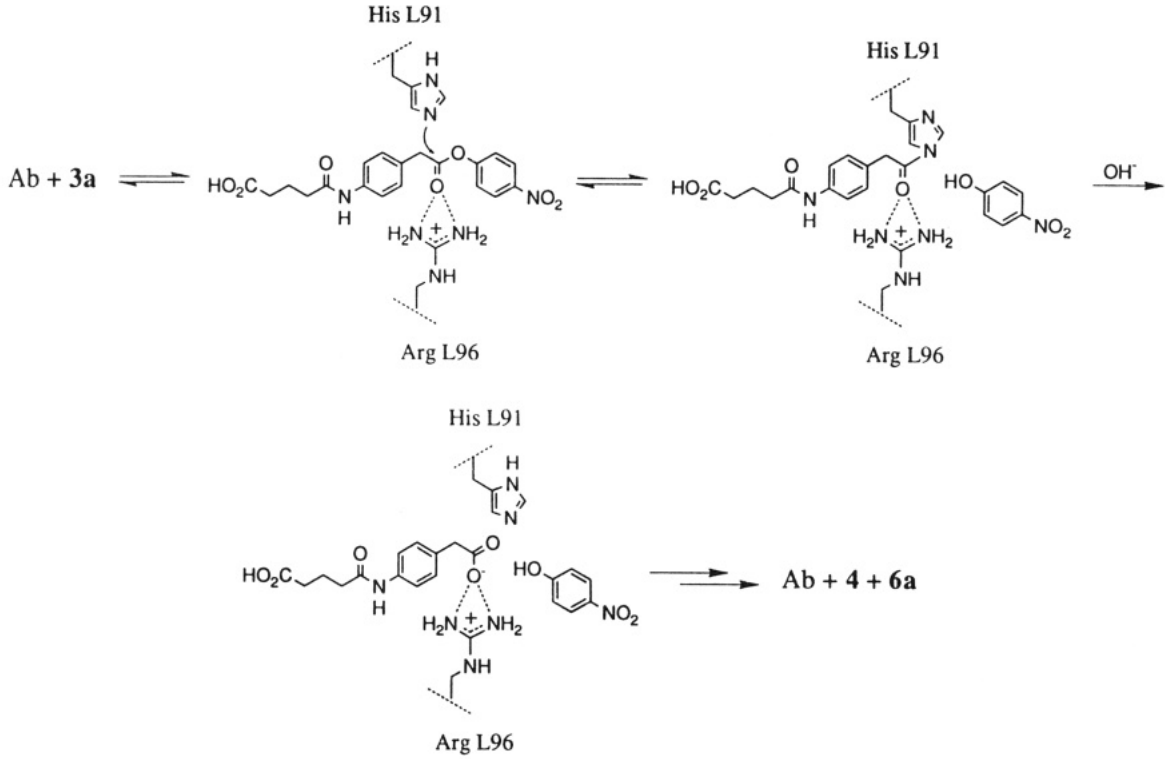


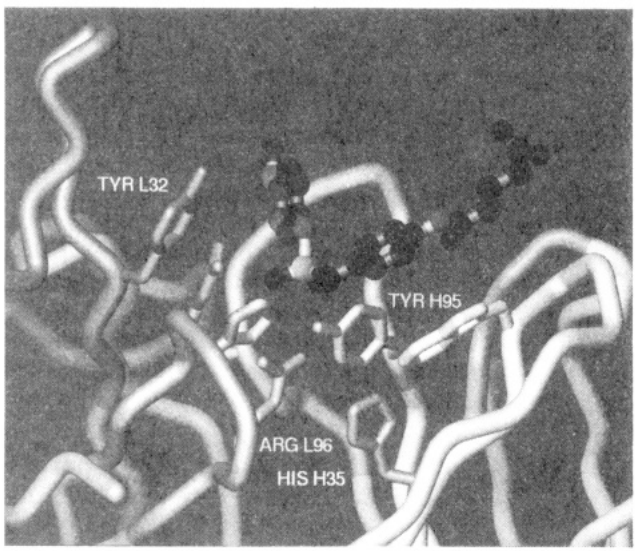


**Figure 1.** Computer model of phosphonamidate 1 (displayed as a ball-and-stick model) bound to the 43C9 Fv fragment. The antibody Cα backbone is presented as tubes with key antibody side chains included. The Arg L96 side chain interacts with the oxygens of the transition-state analog (dark spheres) by hydrogen bonding and electrostatic effects. The side chain of His L91 is located above Arg L96 whereas the other histidine residue—His H35—lies at the bottom of the antigen-binding pocket.

**2** and **3b** catalyzed by 43C9 in both monoclonal antibody and single-chain form were essentially identical.

Substitutions were chosen for both His L91 and Arg L96 to eliminate their potential to participate in catalysis.[15,16] Glutamine was selected as a substitute for His L91 in order to retain some hydrogen-bonding ability at this position in the absence of overt nucleophilic character. Glutamine was also chosen for position L96 since this residue is similar in size and ability to act as a hydrogen-bond acceptor, though it lacks a positive charge. All three proteins—wild type, H-L91-Q, and R-L96-Q—were expressed and isolated in the same manner.

The catalytic activity of the three proteins was assessed by measuring the steady-state kinetic parameters for hydrolysis of *p*-chlorophenyl ester **3b** at pH 8.5. Under these conditions, formation of the putative acyl–antibody intermediate is mainly rate-limiting. As mentioned above, the catalytic parameters for the wild-type single-chain antibody were essentially the same as those for the monoclonal antibody. On the other hand, the catalytic activities of both the H-L91-Q and R-L96-Q mutants were below our detection limits: at least 20-fold below that of the wild type. This low threshold relative to analogous studies with mutants of proteolytic enzymes is a consequence of the modest rate enhancement for ester hydrolysis afforded by 43C9 coupled with a relatively rapid competing spontaneous rate.[5] To verify that the observed lack of catalytic activity was not due to gross deformation of the antigen-binding pocket, the thermodynamic dissociation constants for hapten **1** as well as the products of ester hydrolysis, acid **4**, and *p*-nitrophenol **6a** were determined by direct fluorescence titrations and the data obtained is shown in Table I. The latter ligands were chosen since they represent the two "legs" of the L-shaped hapten and should allow us to localize differences in hapten-binding affinity to specific regions of the antigen-binding pocket.

The esterase and ligand-binding data presented above are consistent with the mechanism shown in Scheme II, illustrated for hydrolysis of the *p*-nitrophenyl ester. In the wild-type protein, an acyl–antibody intermediate linked via histidine L91 is believed to form in a reversible step which favors the starting material. The tetrahedral intermediates lying on either side of this intermediate are stabilized by electrostatic and hydrogen-bonding

(16) Stewart, J. D.; Roberts, V. A.; Getzoff, E. D.; Benkovic, S. J. Unpublished results.

**Table I. Thermodynamic Dissociation Constants for Ligand Binding to Wild-Type and Mutant 43C9 Single-Chain Antibodies**

| | $K_D$ (M) | | |
|---|---|---|---|
| protein | hapten 1 | acid 4 | phenol 6a |
| wild type[a] | $\leq 1 \times 10^{-9}$ | $1.5 \times 10^{-5}$ | $6.0 \times 10^{-7}$ |
| H-L91-Q[a] | $\leq 1 \times 10^{-9}$ | $1.7 \times 10^{-5}$ | $5.3 \times 10^{-7}$ |
| R-L96-Q[b] | $1.6 \times 10^{-8}$ | $3.1 \times 10^{-5}$ | $9.6 \times 10^{-7}$ |

[a] Stewart, J. D.; Benkovic, S. J. Unpublished results. [b] Roberts, V. A.; Stewart, J. D.; Benkovic, S. J.; Getzoff, E. D. *J. Mol. Biol.* **1993**, submitted.

interactions with the side chain of Arg L96. In the case of trypsin and chymotrypsin, such an oxyanion hole is formed by amide groups, either side chain or main chain; on the other hand, an arginine residue is used for this purpose in metalloproteases such as carboxypeptidase.[17] Hydroxide ion is then believed to attack the acyl-antibody to form the antibody–product complex from which the ligands dissociate to complete the catalytic cycle. On the basis of this mechanism, substitution of the His L91 residue with glutamine should not affect the binding of ground states but should abolish catalytic activity. This is exactly what is observed. Likewise, the effect of changing Arg L96 to glutamine should be evident by the loss of transition-state stabilization rather than a weakening of ground-state binding. This is nicely illustrated by the binding data. Changing Arg L96 to glutamine results in the loss of at least 2 kcal/mol of binding affinity for the hapten, but essentially no change in affinities for acid 4 and *p*-nitrophenol. This implies that the side chain of Arg L96 interacts with an element of the hapten that is not present in the products: the charged tetrahedral phosphorus transition-state mimic. It should be noted that Arg L96 is one of eight arginines in the primary sequence of the antibody; the mutagenesis results, in turn, provide support for the veracity of the molecular modeling.

When compared to highly-evolved proteases, 43C9 exhibits both similarities and differences. While the overall organization of its kinetic scheme is similar to that of a serine protease such as chymotrypsin, the antibody lacks some important features found in the proteases. First, 43C9 does not appear to utilize general acid catalysis; the leaving group departs with essentially a full negative charge. This seriously comprises its efficiency on nonactivated substrates which contain leaving groups with $pK_a$ values greater than about 12. Secondly, attack by the nucleophile, in this case a histidine rather than a serine, likewise is not abetted by general base catalysis. Thirdly, product inhibition, particularly by the leaving group, reduces the catalytic efficiency and, in the case of the *p*-nitrophenyl ester hydrolysis product, desorption represents the rate-limiting step.

## Group Transfer

Catalysis of group-transfer reactions (the above example may be viewed as the transfer of an acyl group to water) in general have two mechanistic subtypes: direct group transfer between antibody-bound donor and acceptor substrates or indirect group transfer through intervening covalently bound antibody–donor species.

(17) Phillips, M. A.; Fletterick, R. J. *Curr. Opin. Struct. Biol.* **1992**, *2*, 713–720.

**Scheme III**

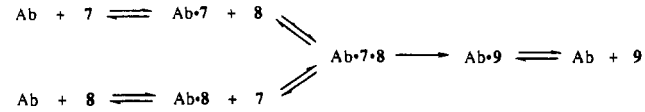


**Table II. Kinetic Constants for Amide Synthesis Catalyzed by 24B11[a]**

| $K_M$ (M) | | | |
|---|---|---|---|
| lactone | diamine | $k_{cat}$ ($s^{-1}$) | $k_{cat}/K_M$ (lactone, $M^{-1}\ s^{-1}$) |
| $4.9 \times 10^{-3}$ | $1.2 \times 10^{-3}$ | $1.2 \times 10^{-8}$ | 0.24 |

[a] Benkovic, S. J.; Napper, A. D.; Lerner, R. A. *Proc. Natl. Acad. Sci. U.S.A.* **1987**, *85*, 5355–5358.

The highly enantioselective aminolysis (>90% ee) of lactone 7 by *p*-phenylenediamine (8) is an example of direct transfer (eq 1).[18] Steady-state kinetic analysis

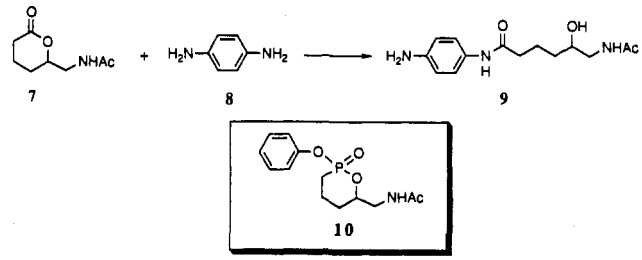


(1)

of this reaction by measurement of the initial velocities of product formation upon variation of either lactone 7 or *p*-phenylenediamine levels in the presence of an antibody, 24B11, revealed a random, equilibrium reaction pattern (Scheme III). Thus binding of the lactone to 24B11 had no effect on the subsequent binding of *p*-phenylenediamine or vice versa, suggesting that the two substrate-binding sites are conformationally independent and do not require substrate induction for their formation. The kinetic analysis also excludes the substantial accumulation of a putative acylated antibody intermediate (between 7•8•Ab → 9•Ab) formed by attack of an active site nucleophile on the carbonyl of the lactone, but it cannot strictly rule out such a species at a steady-state level. Because 24B11, initially induced to the cyclic phosphinate **10**, also catalyzes the cyclization of the hydroxyphenyl ester 11 to the lactone without competing hydrolysis to the acyclic acid,[19] this version of an indirect transfer process is also unlikely (eq 2).

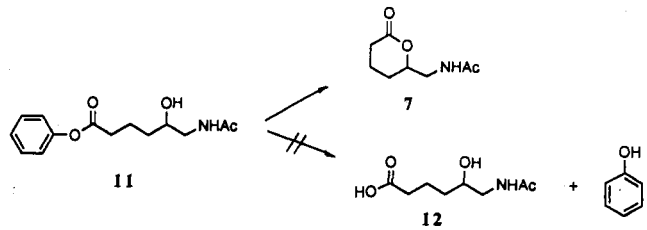


(2)

Aminolysis derives from the tolerance of 24B11 to substitution of the aromatic amine for the phenoxy group within its binding site. The kinetic parameters describing this process are listed in Table II.

(18) Benkovic, S. J.; Napper, A. D.; Lerner, R. A. *Proc. Natl. Acad. Sci. U.S.A.* **1987**, *85*, 5355–5358.
(19) Napper, A. D.; Benkovic, S. J.; Tramontano, A.; Lerner, R. A. *Science* **1987**, *237*, 1041–1043.

**Table III. Kinetic Constants for Transesterifications Catalyzed by 21H3[a]**

| R | | | | $K_M$ (M) ester | $K_M$ (M) alcohol | $k_{cat}$ ($s^{-1}$) | $k_{cat}/K_M$ ($M^{-1}$ $s^{-1}$) ester | $k_{cat}/K_M$ ($M^{-1}$ $s^{-1}$) alcohol |
|---|---|---|---|---|---|---|---|---|
| 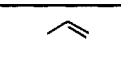 | 15 | X = OH (S) Y = $CH_3$ | 16 | $3.0 \times 10^{-3}$ | $7.3 \times 10^{-3}$ | 0.35 | 120 | 48 |
| 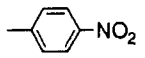 | 18 | X =OH (S) Y = $CH_3$ | 16 | $4 \times 10^{-5}$ | $1.3 \times 10^{-2}$ | $5.5 \times 10^{-3}$ | 140 | 0.42 |
|  | 19 | X = OH (S) Y = $CH_3$ | 16 | $1.9 \times 10^{-4}$ | $5.0 \times 10^{-3}$ | 0.32 | 1700 | 64 |
| 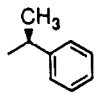 | 17 | X = OH Y =H | 20 | $6.9 \times 10^{-3}$ | $2.0 \times 10^{-3}$ | 0.075 | 11 | 38 |

[a] Wirsching, P.; Ashley, J. A.; Benkovic, S. J.; Janda, K. D.; Lerner, R. A. *Science* 1991, *252*, 680–685.

**Scheme IV**

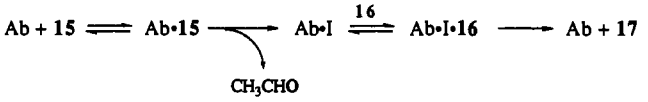


The transesterification of a variety of esters derived from the parent acid (13) by a series of benzyl alcohols[20] catalyzed by antibody 21H3 is an example of indirect group transfer (eq 3). Steady-state kinetic analysis of

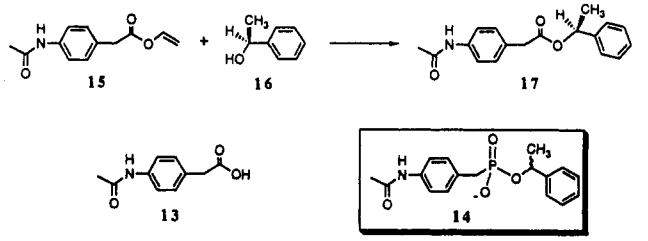


(3)

this reaction by measurement of the initial velocities of ester product 17 formation by varying the concentrations of vinyl ester 15 and (*S*)-*sec*-phenethyl alcohol (16) generated a ping-pong reaction pattern. The data require a discreet acyl–antibody formed by attack of an unidentified nucleophile at the active site of 21H3 on the vinyl ester (Scheme IV). Confirmatory evidence for the presence of Ab–I was obtained by extending the transesterification to include other substrate pairs, e.g. 19 plus 16 and 17 plus benzyl alcohol (20) (Table III). In these additional cases, an apparent ping-pong reaction pattern also was observed. Since such a pattern may also arise from a large difference between the apparent dissociation constants that characterize the two substrates,[21] a direct demonstration of the formation of an acyl–antibody was accomplished with the *p*-nitrophenyl ester 18. Incubation of 18 with varying concentrations of 21H3 rapidly liberated equivalent amounts of *p*-nitrophenol followed by a slower, steady-state release of this product, which was also proportional to the catalyst concentration (Figure 2A).[22] The accurate correlation between the measured concentration of 21H3 and that calculated from the amplitude of the pre-steady-state phase substantiates the existence of a covalent intermediate. As required, the *p*-nitrophenyl ester is also competent in the transesterification reaction.

**Scheme V**

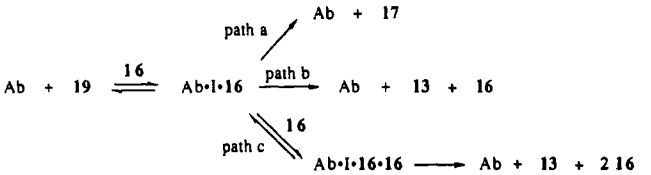


Comparison of $k_{cat}$ for the transesterification of the vinyl and phenyl esters with a common acceptor alcohol (16) reveals the same value (0.33 $s^{-1}$), but for the *sec*-phenylethyl ester 17, $k_{cat}$ decreases by a factor of ca. 5. This kinetic behavior most likely reflects a change in the rate-limiting step from deacylation to acylation of the antibody. Direct measurement of the acylation rate with the more reactive *p*-nitrophenyl ester provided a rate constant of 0.7 $s^{-1}$ at pH 7.0 (Figure 2B), whereas $k_{cat} \approx 5.5 \times 10^{-3}$ $s^{-1}$ so that, overall, deacylation is rate-limiting, as expected. Extrapolation of $k_{cat}$ to pH 9.0 for this substrate furnishes a value of 0.55 $s^{-1}$ in satisfactory agreement with the interpretation of data for the vinyl and phenyl esters.

Substitution of *sec*-phenethyl alcohol with the respective chloride and bromide up to their solubility limits increases the rate of hydrolysis of the vinyl ester by approximately an order of magnitude over its hydrolysis rate observed in the absence of an alcohol acceptor. These observations prompted a closer examination of the actual partitioning of the acyl–antibody intermediate between alcoholysis (by *sec*-phenethyl alcohol) and hydrolysis. The measurements of ester 17, phenol, and acid 13 formation from phenyl ester 19 as a function of varying levels of *sec*-phenethyl alcohol indicated that, up to approximately 12 mM alcohol, the acyl intermediate partitioned in an ca. 1:1 ratio between transesterification and hydrolysis (Scheme V, paths a and b).[23] At higher levels of alcohol, the partitioning to the acid hydrolysis product increased at the expense of ester formation (2:1) (presumably via path c). The observations are suggestive of an initial binding site for the acceptor alcohol which can be

(20) Wirsching, P.; Ashley, J. A.; Benkovic, S. J.; Janda, K. D.; Lerner, R. A. *Science* 1991, *252*, 680–685.
(21) Cleland, W. W. *The Enzymes*; Boyer, P. D., Ed.; 1970; Vol. 2, Chapter 1.
(22) Hartley, B. S.; Kilby, B. A. *Biochem. J.* 1954, *56*, 288.
(23) Stewart, J. D.; Benkovic, S. J. Unpublished results.

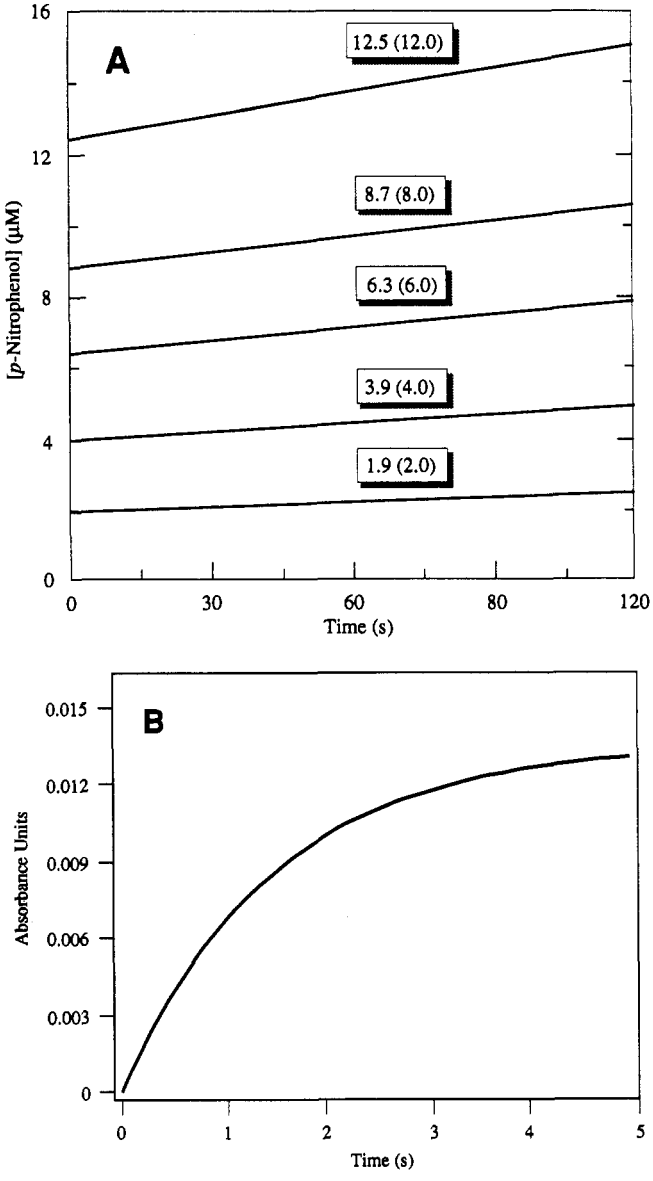


**Figure 2.** (A) The steady-state liberation of *p*-nitrophenol during the reaction of 21H3 with ester 18 (pH 7.0, 23 °C). The values outside the parentheses correspond to the observed (intercept) concentrations of 21H3 from the amplitude of the initial fast phase; values within the parentheses are the measured concentrations of 21H3. (B) The pre-steady-state exponential phase of the acylation of 21H3 by ester 18.

saturated ($K_D \approx 5$ mM). Ligand binding at this site increases the reactivity of the acyl intermediate, akin to the induced fit of substrates described for the enzyme-catalyzed process.[24] Binding of a second molecule of alcohol appears to be required to explain the change in the partitioning ratio at concentrations of 12–20 mM, reminiscent of the action of an allosteric modulator on enzyme activity.

Antibody 21H3, like 24B11, was originally induced for another purpose, in this case to act as an *S*-specific esterase with the phosphonate 14 hapten chosen as a model of a tetrahedral intermediate. It is probable that its esterase activity likewise involves an acyl intermediate. If the original intent, however, were to catalyze transesterification, the logical choice would have been a triester of 14 as a rough mimic of a bipyramidal species expected in a nucleophilic displacement process. Since

(24) Koshland, D. E. *Proc. Natl. Acad. Sci. U.S.A.* **1958**, *44*, 98.

**Table IV. Isoaspartate versus Aspartate Product Ratios for RG2 Antibodies**[a]

| antibody | isoasp/asp product ratio | |
|---|---|---|
| | L-isomer | D-isomer |
| 39F3 | 8.3 | 3.6 |
| 14A8 | 3.4 | 1.4 |
| 23C7 | 16.4 | 1.2 |
| 40H4 | 1.9 | 5.7 |
| 2E4 | 2.4 | 4.7 |
| 24C3 | 2.1 | 4.8 |

[a] Gibbs, R. A.; Taylor, S.; Benkovic, S. J. *Science* **1992**, *258*, 803–805.

14 can only sculpt two binding regions for alkyl or aromatic residues, the observation of transesterification promoted by 21H3 would appear to mandate a ping-pong type mechanism. Since one of the lessons gleaned from our study of enzyme mechanisms is the logic for gaining catalytic efficiency by subdividing a reaction course into a series of steps, hapten design to command indirect transfer mechanisms should be explored.

## Consecutive Reactions

One alluring aspect of the catalytic antibody area is the opportunity to design catalytic systems that have no enzymic counterparts and surpass present macromolecular assemblies in their specificity and versatility. Consecutive reactions, and for that matter all stepwise reactions, present the need to encounter and stabilize more than one transition state. The antibody conversion of the asparaginylglycine *N*-phenethylamide (**22**) to the intermediate succinimide **23** and the subsequent hydrolysis of the latter to the aspartate **24** and isoaspartate **25** products serves as a prototype (Scheme VI). The inducing hapten, in this case cyclic phosphinate **21**, contained two tetrahedral transition-state mimics (the phosphinate and secondary alcohol surrogates) in order to create binding sites within the antibody for processing the anticipated tetrahedral species forming at either carbonyl in **22** and **23**.

Two classes of antibodies were identified (Table IV): those that catalyze only the succinimide hydrolysis and those that catalyze both the deamidation and the succinimide hydrolysis (2E4 and 24C3).[25] The first class could be further subdivided into three groups: those selective for the D-succinimide (14A8), those selective for the L-succinimide (39F3), and those that catalyze the hydrolysis of both isomers (23C7 and 40H4). This stereochemical versatility derives in part from induction with racemic hapten as well as the bifunctionality of the hapten. The ability of the antibodies to catalyze the succinimide hydrolysis was demonstrated by changes in the isoaspartate/aspartate product ratio to values either greater or less than the normal background ratio of 3.6 as well as direct kinetic measurements of succinimide hydrolysis.

The full time course kinetics for hydrolysis of **23** catalyzed by the antibody 23C7 were studied as an example of the first class of antibodies, and the data were fit by a computer simulation to Scheme VII using the constants listed in Table V.[26] The pH rate profiles for these hydrolyses were simply first-order in hydroxide

(25) Gibbs, R. A.; Taylor, S.; Benkovic, S. J. *Science* **1992**, *258*, 803–805.

(26) Liotta, L. J.; Benkovic, P. A.; Miller, G. P.; Benkovic, S. J. *J. Am. Chem. Soc.* **1993**, *115*, 350–351.

**Scheme VI**

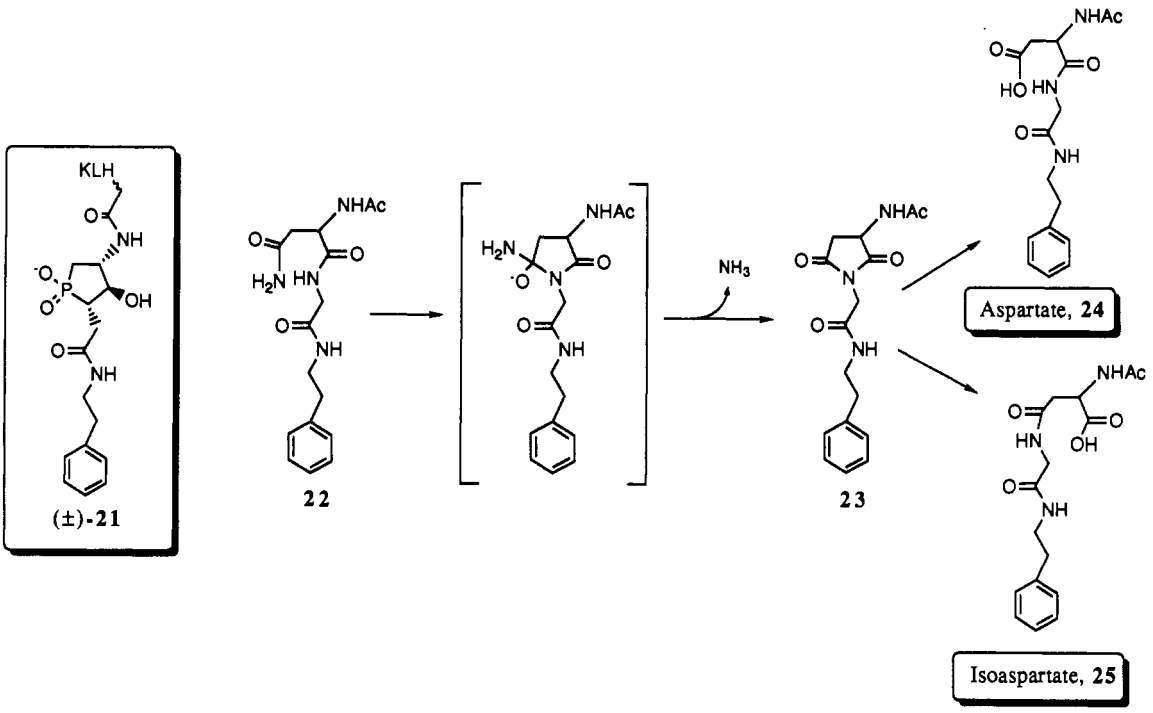


**Scheme VII**

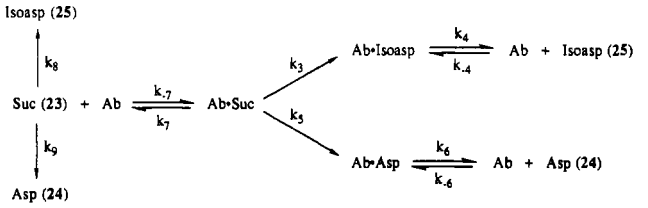


**Table V. Kinetic Constants for 23C7-Catalyzed Succinimide Hydrolysis[a,b]**

| rate constant | D-succinimide | L-succinimide |
|---|---|---|
| $k_7/k_{-7}$ | $2.4 \times 10^{-7}$ M | $8.3 \times 10^{-7}$ M |
| $k_3$ (isoasp) | $8.7 \times 10^{-3}$ s$^{-1}$ | $5.83 \times 10^{-2}$ s$^{-1}$ |
| $k_5$ (asp) | $9.3 \times 10^{-3}$ s$^{-1}$ | $2.0 \times 10^{-3}$ s$^{-1}$ |
| $k_4/k_{-4}$ (isoasp)[c] | $2.4 \times 10^{-7}$ M | $2.5 \times 10^{-7}$ M |
| $k_6/k_{-6}$ (asp)[c] | $1.4 \times 10^{-7}$ M | $1.0 \times 10^{-7}$ M |
| $k_3/k_8$ | 70 | 490 |
| $k_5/k_9$ | 290 | 62 |

[a] Kiotta, L. J.; Benkovic, P. A.; Benkovic, S. J. Unpublished results. [b] All values ±10%. [c] Determined by fluorescence titration.

ion, implying direct hydrolysis and no involvement of an antibody-bound intermediate.[27] The lack of $H_2{}^{18}O$ incorporation into the starting succinimide when the reaction was run to 50% completion indicated that its hydrolysis was irreversible.[27] The antibody designated 2E4 served as an example of the second class of catalysts (those that catalyze both deamidation and succinimide hydrolysis). Steady-state kinetic parameters for the deamidation are listed along with those for succinimide hydrolysis in Table VI.

Both 2E4 and 23C7 catalyze the hydrolysis of both the D- and L-succinimides to both the aspartate **24** and isoaspartate **25** products; however, 23C7 is more effective by factors of 3–15 (compare $k_3/k_8$ and $k_5/k_9$). Antibody 2E4 selectively hydrolyzes the D-isomer of **22**, and it accelerates the rate of hydrolysis by ca. 35-fold over the background. The fact that $k_3$ and $k_5$ are

(27) Liotta, L. J.; Benkovic, S. J. Unpublished results.

**Table VI. Kinetic Constants for D- and L-Asn-Gly Deamidation by 2E4[a]**

| kinetic constant | D-Asn-Gly | L-Asn-Gly |
|---|---|---|
| $K_M$[b] | $1.93 \times 10^{-4}$ M | |
| $k_{cat}$[b] | $1.2 \times 10^{-4}$ s$^{-1}$ | |
| $k_7/k_{-7}$[c] | $2.8 \times 10^{-5}$ M | $3.6 \times 10^{-6}$ M |
| $k_3$ (isoasp)[c] | $3.8 \times 10^{-3}$ s$^{-1}$ | $1.4 \times 10^{-3}$ s$^{-1}$ |
| $k_5$ (asp)[c] | $6.0 \times 10^{-4}$ s$^{-1}$ | $1.3 \times 10^{-3}$ s$^{-1}$ |
| $k_4/k_{-4}$ (isoasp)[c,d] | $3.3 \times 10^{-6}$ M | $6.0 \times 10^{-7}$ M |
| $k_6/k_{-6}$ (asp)[c,d] | $1.9 \times 10^{-6}$ M | $1.8 \times 10^{-7}$ M |
| $k_{cat}/k_{uncat}$ | 35[b] | 2.1[c] |
| $k_3/k_8$[c] | 32 | 12 |
| $k_5/k_9$[c] | 18 | 41 |

[a] All values ±10%. [b] Gibbs, R. A.; Taylor, S.; Benkovic, S. J. *Science* **1992**, *258*, 803–805. [c] Liotta, L. J.; Benkovic, P. A.; Benkovic, S. J. Unpublished results. [d] Determined by fluorescence titration.

greater than $k_{cat}$ for 2E4 when coupled with its micromolar affinity for the succinimide prevents detectable accumulation of the free succinimide intermediate.

The stereospecificities and reactivity patterns for 2E4 and 23C7 have been rationalized in terms of a bifunctional binding site model constructed to the D-isomer of the hapten **21**. This model presumes that the linker of the conjugated hapten should protrude from the antibody binding site and that the phosphinate binding site should be more catalytically active than the secondary alcohol site. Both the D- and L-succinimides were docked within a hypothetical binding cleft (Figure 3A), and the hydrolytic reactivity at either carbonyl was analyzed. On one hand, formation of the aspartate product should be favored for the D-isomer (Figure 3B), although this is offset by the intrinsically 4-fold greater rate of isoaspartate synthesis owing to the electronic effect of the $\alpha$-*N*-acetyl substituent. On the other hand, formation of the isoaspartate product should be favored for the L-isomer (Figure 3C), and this is strengthened by the intrinsic electronic effect. Comparison of the appropriate rate coefficients in Table V indicates that the charged phosphinate moiety is 6–8-fold more

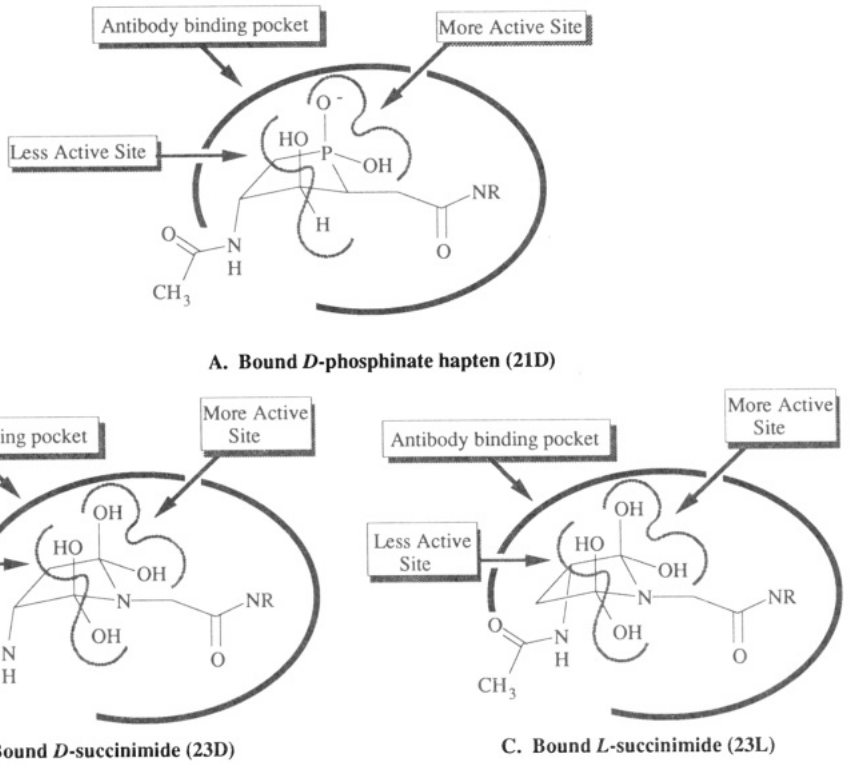


A. Bound *D*-phosphinate hapten (21D)

B. Bound *D*-succinimide (23D)

C. Bound *L*-succinimide (23L)

**Figure 3.** Binding of D- and L-asparaginylglycine *N*-phenethylamide (**22**) to the catalytic pocket of antibody 23C7 that was generated to bifunctional phosphinate **21**.

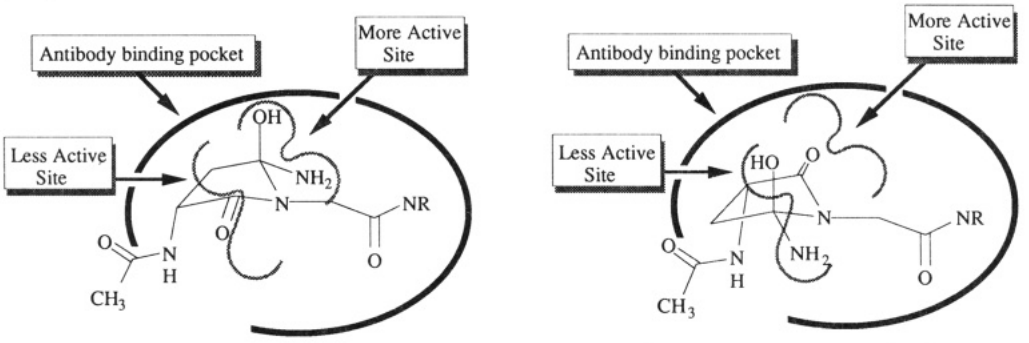


A. Bound *D*-Asn-Gly-Phen (22D)

B. Bound *L*-Asn-Gly-Phen (22L)

**Figure 4.** Binding of D- and L-asparaginylglycine *N*-phenethylamide (**22**) to the catalytic pocket of antibody 2E4 that was generated to bifunctional phosphinate **21**.

effective in inducing a catalytic site than a secondary alcohol. This model also rationalizes the preference of 2E4 for cyclization of the D- rather than the L-peptide, as the amide to be deaminated occupies the more active phosphinate site (Figure 4). Thus, the results clearly illustrate that a bifunctional transition analog induces antibodies that effectively deal with the problem of multiple transition states.

## Conclusion

For the reader knowledgeable about the field of mechanistic enzymology, the striking parallels between catalytic antibodies and enzymes in terms of how chemical transformations are achieved may come as no surprise. What is particularly remarkable, however, is that this single protein motif (all antibodies possess the same secondary and tertiary structure) can be adapted to accommodate diverse reaction types with noteworthy catalytic efficiency.[1-3]

No review would be complete without a brief comment on the present catalytic efficacy of antibodies and the opportunities for improvement. There are various indices to assess catalytic efficiency; in the absence of an appropriate spontaneous reaction (as is the case of the transesterification reaction), the ratio $k_{cat}/K_M$ is the most rigorous. This ratio represents a measure of the kinetic barrier encountered commencing with the combination of the antibody and the substrate and proceeding along the reaction coordinate to the transition state of highest energy. For proteins of this molecular weight, the upper limit for $k_{cat}/K_M$ is ca. $10^7$ $M^{-1}$ $s^{-1}$, the value for a diffusional encounter of the substrate and protein. For antibodies 43C9, 24B11, 21H3, and 23C7, the values of $k_{cat}/K_M$ are $4.7 \times 10^5$ (**3a**, pH 9.3), 0.24 (**7** + **8**, pH 7.0), $1.7 \times 10^3$ (**16** + **19**, pH 9.0), and $7 \times 10^5$ $M^{-1}$ $s^{-1}$ (L-**23**, pH 8.35), respectively. We have shown elsewhere in depth that a high $k_{cat}/K_M$ ratio alone is insufficient for achieving multiple substrate turnovers, but for the antibody, at least a 10-fold weaker product affinity relative to substrate binding is necessary.[9] Since transition-state analogs invariably contain elements of the desired product, inhibition by the

accumulating product has often occurred at low levels of substrate conversion. Clearly changes in transition-state analog design or through the use of substrates that are not spatially congruent with the mimic at atoms remote from the reaction center are desirable.[28]

Finally, improvement may also be achieved by mutagenesis of specific amino acids, by replacing entire loop regions of the antibody or by recruiting catalytic cofactors. Site-directed mutagenesis on 43C9 suggests that catalytic antibodies induced to a transition-state mimic already possess several elements necessary for efficient turnover, namely the high stereospecificity of a programmed active site binding pocket, the entropic gain associated with the binding of a substrate which converts the chemical transformation to an intramolecular reaction, and appropriately juxtaposed side chain residues that can act as nucleophilic or electrophilic catalysts. Since catalysis results from the simultaneous temporal confluence of cooperative interaction between elements on the substrate and the abzyme active site, we envision enriching the abzyme's active site not only by mutagenesis techniques but also through inclusion of auxiliary catalysts such as metal ions. The trick and the challenge is to achieve access to the precise positioning between substrate and active site residues necessary for increased catalytic function.

(28) Lerner, R. A.; Benkovic, S. J. *BioEssays* **1988**, *9*, 107–112.

*We thank Dr. Victoria Roberts for supplying the photograph of Figure 1. We also gratefully acknowledge the Office of Naval Research for financial support (N00014-91-J-1593), the National Institutes of Health for a postdoctoral fellowship to L.J.L. (5F32 GM 14013-03), and the Helen Hay Whitney Foundation for a postdoctoral fellowship to J.D.S.*